Theor Chem Acc (2007) 117: 283–290
DOI 10.1007/s00214-006-0135-z

REGULAR ARTICLE

Stephen D. Williams · Timothy J. Johnson
Thomas P. Gibbons · Christopher L. Kitchens

Relative Raman intensities in C_6H_6, C_6D_6, and C_6F_6: a comparison of different computational methods

Received: 30 June 2005 / Accepted: 6 January 2006 / Published online: 23 June 2006

Abstract The accuracy of various computational methods (Hartree–Fock, MP2, CCSD, CAS-SCF, and several types of DFT) for predicting relative intensities in Raman spectra for C_6H_6, C_6D_6, and C_6F_6 was compared. The predicted relative intensities for ν_1 and ν_2 were compared with relative intensities measured by an FT-Raman spectrometer. While none of these methods excelled at this prediction, Hartree–Fock with a large basis set was most successful for C_6H_6 and C_6D_6, while PW91PW91 was the most successful for C_6F_6.

Keywords Relative Raman intensity · Ab initio · Hartree–Fock · MP2 · DFT · CCSD · CAS-SCF · Fourier Transform Raman · FT-Raman

1 Introduction

The assignment of Raman spectra, even for small-sized molecules, is not a simple task. Quantum mechanically computed vibrational frequencies can provide significant help in this task, since the typical errors and empirical corrections for these calculated frequencies are well known [1]. However, frequencies may not be enough to completely assign the spectrum, for example, when a weak fundamental is near a combination or overtone. Quantum mechanically computed Raman intensities may be quite helpful in such cases, particularly if their reliabilities are known. There have been several studies of computed Raman intensities compared to experiment; these have focused on one of a few methods or basis sets, and have not attempted to survey several different methods of computation. These studies include Hartree–Fock methods for ethylene [2], benzene [3], HFCs [4], and triptycene [5]; DFT methods for N_2, HF, and ethane [6], as well as water, ammonia, and methane [7]; and hybrid DFT methods for azulene [8], porphine [9], PAHs [10], aniline and its radical cation [11], benzene [12], acetone [12], propionitrile [12], other small molecules [12], fatty acids [13,14], and porphyrins [15,16]. Quite recently, Michalska and Wysokinski [17] used DFT methods to predict Raman intensities for *cis* platin and related species; they present nice qualitative agreement with measured spectra, but do not have quantitative comparisons of predicted and measured intensities. While some of these (small molecule) studies compare the computed Raman intensities with measured absolute Raman activities or cross sections, most compare the computed intensity to an experimental Raman spectrum, and in most of these cases, the comparison is made to an intensity-uncorrected spectrum. As McCreery [18] points out in his excellent review, not correcting for the spectrometer's response can dramatically distort a Raman band's intensity. It is thus difficult to gauge the merit of the theoretical to experimental intensity comparisons of some of these reports. Shinohara et al. [10] do make comparisons with corrected spectra, but they do not include the C–H stretching bands. Oakes et al. [12] have recently compared hybrid DFT computed Raman intensities with corrected experimental intensities (although it is not clear if the spectrometer used measured intensity as power or if it used photon counting) for several small molecules, including benzene; like Shinohara et al. [10] they did not include the C–H stretching region.

We have chosen to compare computed relative Raman intensities with accurately measured relative intensities, using several methods including Hartree–Fock, correlated - ab initio (MP2, CCSD, CAS-SCF), pure DFT (PW91PW91), and hybrid DFT (B3LYP, B3PW91, BB1K). In order to be as certain as possible that we were comparing intensities of correctly assigned modes, we considered the two a_{1g} modes of C_6H_6, C_6D_6, and C_6F_6, all belonging to the D_{6h} point group. These modes are ν_1, the totally symmetric C–X stretching mode, and ν_2, the totally symmetric ring C–C stretch; they are readily assigned due to their strongly polarized nature. We assess the quality of a computational method on how well it reproduces the experimental ratio of the corrected relative

S. D. Williams · T. P. Gibbons · C. L. Kitchens
A. R. Smith Department of Chemistry,
Appalachian State University, Boone, NC 28609, USA

T. J. Johnson (✉)
Battelle Pacific Northwest National Laboratory,
P.O. Box 999 Mailstop K8-88, Richland, WA 99352, USA
E-mail: Timothy.Johnson@pnl.gov

intensities of these modes, $I(\nu_1)/I(\nu_2)$, since determining absolute Raman cross sections is not a common measurement and our intent is to provide practical advice to spectroscopists who wish to use computations to assist in assigning spectra. We also show comparisons of theoretically simulated spectra with corrected experimental spectra of a few other small molecules.

2 Experimental

Fourier transform Raman spectra of liquids were measured with an FT-Raman spectrometer using 1,064 nm excitation and 2 cm^{-1} resolution. 180° backscattered light was collected, typically averaging 512 interferograms. Double-sided interferograms were collected, zerofilled by a factor of four, and phase corrected using the Power method. Polarized spectra were also collected, typically measured with 4 cm^{-1} resolution. The spectra of the neat liquids were recorded using a Bruker FRA 106 Raman module coupled to the interferometer of a Bruker IFS 66v/S vacuum Fourier infrared spectrometer. A similar FTIR spectrometer has been previously described [19], using the methods suggested by IUPAC [20]. The 106 Raman accessory consists of a CW 1.064 μm Nd:YAG laser with a focused or unfocused laser spot and with either 90° or 180° backscatter spectral light collection. The neat liquid samples were obtained from Aldrich and typically were at least of 99.9% purity. The C_6D_6 had a stated isotopic purity of 99.6% D. $^{13}C_6H_6$ was obtained from Isotec Incorporated and had a stated isotopic purity of 99% ^{13}C.

As described by Simon and colleagues [21], a notch filter in the FRA 106 removes the Rayleigh scattered photons; the Raman-scattered light is modulated by the FTIR interferometer and focused onto a sensitive liquid-nitrogen cooled Ge detector [22]. In the present case, the interferometer's wavelengths are referenced to those of the HeNe laser. These were calibrated in the near-IR by using a white light source and the $2 \leftarrow 0$ overtone transition of ~22-Torr of neat carbon monoxide [23] in a 10 cm cell and adjusting the spectrometer's measured wavelengths (via the HeNe frequency) to match those of the HITRAN database [24]. To calibrate the Nd:YAG laser wavelength and thus the Raman scattered frequencies, a strong scatterer, elemental sulfur, was used and the laser wavelength empirically shifted such that the Stoke's and anti-Stoke's Raman shifts were equal to within 0.2 cm^{-1} for a few of the strongest lines.

Calibration of the scattering intensity as a function of wavelength is somewhat more complicated. The Raman module has a 3,000 K white light source whose intensity is scattered into the spectrometer off a NIST-traceable Spectralon surface mounted at the sample position. The instrument response function as a function of wavelength is then generated by ratioing this spectrum relative to the intensity predicted by Planck's law for a 3,000 K source. Subsequent spectra are then multiplied by the (frequency dependant) scaling factor. The quality of the intensity correction was assessed by measuring the intensities in the corrected Stokes and anti-Stokes spectra; the relative intensities were within a few percent of the expected value (Ref. [25], Eq. 4.36). As McCreery [18] has pointed out, obtaining Raman intensity values that correlate even on a relative scale, i.e. that properly ratio out the instrumental response, is more challenging than first supposed.

For polarization experiments the natural polarization of the laser was used. A reducing Jacquinot stop and a calcite Glan-Taylor analyzer (i.e. cross-polarizer) were placed after the Raman notch filter at the focal position of the interferometer's collimator mirror. Perpendicular and parallel orientations were obtained by rotating the analyzer to the 0° and 90° positions. The method was verified by measuring the parallel and perpendicular spectra of CCl_4 whose depolarization ratio is known [26]. The depolarization ratios of natural isotope benzene, particularly the symmetric C–H stretching and ring breathing modes, have also been reported and were reproduced [26,27].

Relative intensities of the two a_{1g} stretching modes (ν_1, C–X stretch ($X = H, D$ or F) and ν_2, C–C stretch) were determined by fitting the appropriate intensity to a pseudo-Voigt lineshape function [28]:

$$I(\nu) = A\left[(1-\eta)\frac{\exp\left(\frac{-(\nu-\nu_0)^2}{w^2}\right)}{w\sqrt{\pi}} + \frac{\eta w}{2\pi\left((\nu-\nu_0)^2+\frac{w^2}{4}\right)}\right] \quad (1)$$

In this four parameter function the intensity is I, the peak area is A, the full width at half maximum is w, the peak center is ν_0, and η is the fraction the Lorentzian contributes to the peak. Sigmaplot was used for the curve fitting. Ratios of the resulting areas were then compared to corresponding theoretical values for C_6H_6, C_6D_6, and C_6F_6. We also measured the spectrum of $^{13}C_6H_6$ but did not include this in the analysis due to the extensive Fermi resonance perturbation of the C–H stretching modes [29].

The computations were carried out with Gaussian98 [30] on an Intel PC and Gaussian03 [31] on an SGI altix computer. The default basis sets in Gaussian were used except for a few calculations with Truhlar's MG3 [32–34] basis set. For each calculation, the molecular geometry was optimized followed by a frequency calculation. The geometry was constrained to have D_{6h} symmetry during the optimization. For C_6F_6 some MP2 constrained optimizations yielded structures with a single imaginary frequency associated with an out-of-plane motion of alternate C atoms. This problem was only observed with large Pople basis sets (6-311+G(3df,2p)), and did not occur when Dunning correlation consistent basis sets [35] were used. For the Hartree–Fock, DFT, and MP2 calculations described here the automatic methods in Gaussian were used to compute the Raman activities (keyword: freq=Raman), but for other calculations (CCSD and CASSCF) this automatic method was not available. What appears in the Gaussian output as the Raman activity is $\left\{45\left(\alpha'\right)_k^2 + 7\left(\gamma'\right)_k^2\right\}/45$ (following the notation of Long [25]). Here $\left(\alpha'\right)_k^2$ is the square magnitude of derivative of the isotropic part of

the polarizability tensor with respect to the kth normal mode, and $(\gamma')_k^2$ likewise for the anisotropic part of the polarizability, where the derivatives are evaluated at zero displacement. (The factor of 7 is for the commonly used 90° scattering; for 180° scattering a factor of 4 appears instead. Although our measurements used 180° scattering, the distinction is not important since $(\gamma')_k^2$ is zero for a_{1g} modes in D_{6h} symmetry.) For the CCSD and CAS calculations the normal modes (included in the Gaussian freq=hpmodes output) for the two a_{1g} modes were used to generate a series of molecular structures displaced along the mass weighted normal mode (using the reduced mass reported by Gaussian). The polarizability tensor components were then computed for each of these and numerical differentiation was used to estimate the polarizability derivatives; these were then used to calculate the needed polarizability tensor invariants for the Raman activities, following standard methods [25]. This numerical method was also applied to a few Hartree–Fock and hybrid DFT calculations; the Raman activities derived from these point-by-point polarizability curves differed by at most a few percent from the automatic ones for the same calculation.

The CAS-SCF calculations used a (6,6) CAS (six electrons distributed in a six orbital complete active space) where the active space included the 6π MOs composed primarily of the $2p_z$ C atom AOs. A series of single point calculations starting with sto-3g and gradually increasing to the largest basis set was used to ensure that the correct orbitals were used in the highest level CAS; visualization of these orbitals with GaussView confirmed this.

3 Results

There are two strong fundamental C–H stretching modes in the Raman spectrum of benzene; these are usually denoted by ν_1 and ν_{15} of a_{1g} and e_{2g} symmetry, respectively [36], although other notations are sometimes used [37]. These bands overlap in spectra of room temperature samples, to the extent that recent [37] absolute Raman scattering cross section measurements of benzene vapor have reported the sum of the cross sections for these modes. For our intensity measurements we need the contribution to the total intensity for ν_1 only. The pseudo-Voigt curve fitting procedure is successful in resolving these two contributions, as shown in Fig. 1.

In this case R^2 statistic was 0.9998. The fits for the other modes and species were not always this good, but in all cases the R^2 statistic was greater than 0.992. A particularly challenging fit was for ν_1 in C_6F_6. This band is quite weak (weaker than some overtones in the spectrum) and is complicated by the presence of an isotopic band and a broad underlying peak. The area was found to be 2.7 ± 0.5 with $R^2 = 0.998$. Note that the intensity for ν_1 in C_6F_6 is about 1% of that for ν_1 in C_6H_6. This large change in intensity is likely due to the much reduced polarizability of F atoms and C–F bonds compared to H atoms and C–H bonds. The fit for this band is shown in Fig. 2.

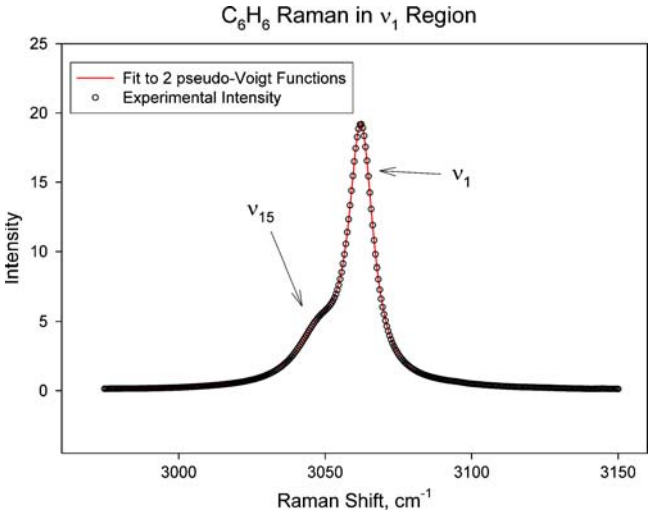

Fig. 1 Experimental Raman intensities (corrected for spectrometer response) for liquid benzene in the CH stretch region, $2\,cm^{-1}$ resolution. The *solid line* is a fit to two pseudo-Voigt lineshapes. R^2 for the fit was 0.9998 and the area for υ_1 was 279 ± 1

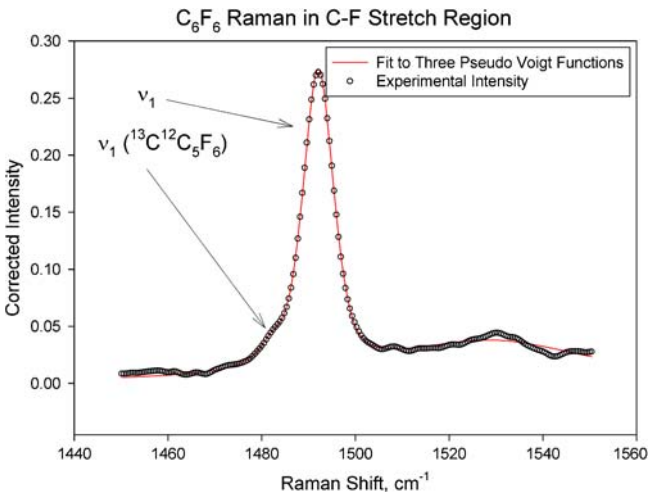

Fig. 2 Experimental Raman intensities (corrected for spectrometer response) for liquid C_6F_6 in the CF stretch region, $2\,cm^{-1}$ resolution. The *solid line* is a fit to three pseudo-Voigt lineshapes. R^2 for the fit was 0.998 and the area for υ_1 was 2.7 ± 0.5

The intensity of ν_1 in the C_6F_6 Raman spectrum is quite weak and is of similar intensity to an overtone band that is somewhat close in frequency. Since both of these are totally symmetric they have the same polarization properties and polarization measurements thus did not help in confirming the assignment for ν_1. We confirmed the assignment of ν_1 by noting that the nearby totally symmetric mode was at nearly exactly twice the frequency of a forbidden (b_{2g}) fundamental (ν_7), and that the observed isotopic shift in frequency upon substitution of a single ^{13}C atom was in near perfect agreement with the predicted isotopic shift for ν_1 computed at the B3LYP/6-311+g(3df) and MP2/ccpVTZ levels of theory. This isotopic band is not observed in the spectrum of C_6H_6; its appearance in the C_6F_6 spectrum is a consequence much larger atomic mass of fluorine compared

to hydrogen, resulting in much larger motion of the C atoms in ν_1 in C_6F_6 compared to C_6H_6. Our assignment of the C_6F_6 Raman spectrum is shown in Fig. 3, and agrees well with previous assignments [38–41].

The Raman spectrum for $^{13}C_6H_6$ (all Carbon 13) was planned for this study but it turned out not to be suitable for measuring intensities for ν_1, due to Fermi resonance with overtones. υ_{16} is a Raman active mode of e_{2g} symmetry; its overtone is a_{1g} and near to υ_1 so it can be in resonance with υ_1. This resonance perturbs the intensities of the CH stretching modes in a way that is not simple to correct. The Fermi resonance-perturbed C–H stretching region is much more complicated for $^{13}C_6H_6$ compared to C_6H_6 as shown in Fig. 4.

We considered C_6H_6 as a test case, since Ozkabak et al. [3] had good results with Raman intensities computed at the

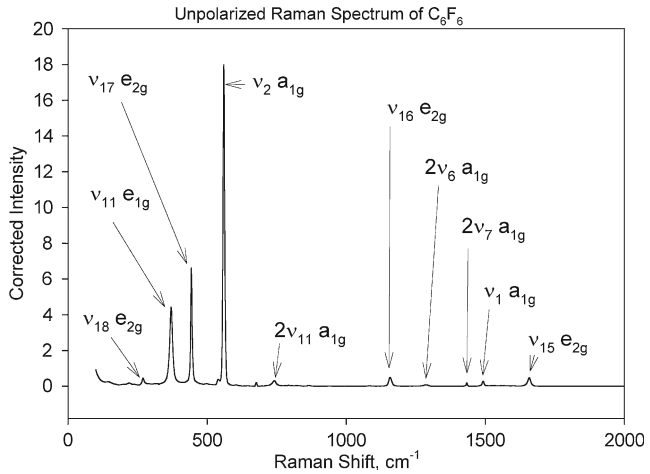

Fig. 3 Assigned Raman spectrum of neat liquid C_6F_6, 2 cm^{-1} resolution. Intensities were corrected for spectrometer response. Designation and symmetry species of assigned peaks are indicated

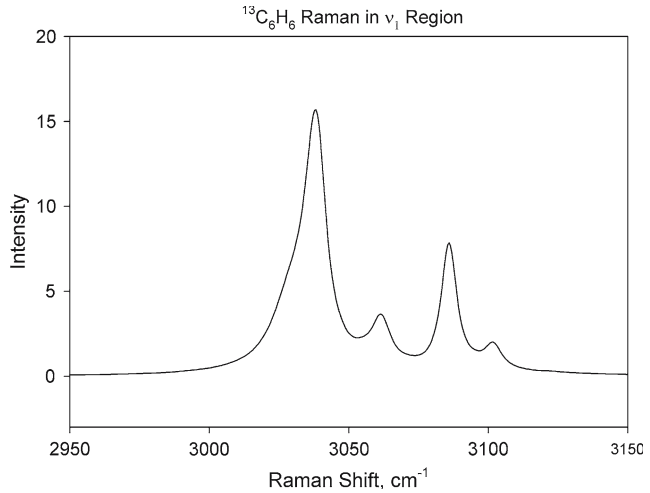

Fig. 4 Experimental Raman intensities (corrected for spectrometer response) for liquid ^{13}C benzene in the CH stretch region, 2 cm^{-1} resolution, showing effect of Fermi resonance (compare to Fig. 1)

Hartree–Fock level for this compound. Methods that seemed relatively poor for C_6H_6 were not used to predict intensities for C_6D_6 and C_6F_6. We compared the experimental intensity ratio $I(\nu_1)/I(\nu_2)$ (ratio of areas from the curve fitting) with the predicted intensity ratio from a given level of theory. As mentioned previously, Gaussian does not predict the Raman intensity, rather it predicts the Raman activity. As McCreery [18] has pointed out, the intensity of a Raman band has contributions from three sources: a part that is intrinsic to the scattering molecule (this is Gaussian's Raman activity), a part that depends on temperature (which affects the population of the scattering vibrational state), and a part that is dependent on the exciting laser frequency and the type of photometric detection in the Raman spectrometer. In the notation of Long [25], this intensity for 90° scattering, Stokes shift, and power detection (as opposed to photon counting), is proportional to [3,18,25]

$$I = \frac{N(\bar{\nu}_0 - \bar{\nu}_k)^4\left\{45(\alpha')_k^2 + 7(\gamma')_k^2\right\}Q_k^2 P}{\left[1 - \exp\left(\frac{-hc\bar{\nu}_k}{kT}\right)\right]45} \tag{2}$$

where N is a proportionality constant, $\bar{\nu}_0$ is the exciting laser wavenumber, $\bar{\nu}_k$ is the wavenumber of the vibrational mode, c is the speed of light, h and k are Planck's and Boltzmann's constants, T is the temperature, P is the exciting laser irradiance, $(\alpha')_k^2$ is the squared derivative of the isotropic part of the polarizability tensor with respect to the kth normal mode, evaluated at zero displacement, and $(\gamma')_k^2$ is similarly the squared derivative of the anisotropic part. Q_k^2 is an amplitude factor: in a classical description of Raman scattering it represents the squared amplitude of vibrational motion for mode k. If the vibrations are treated classically, this amplitude can be related to the total vibrational energy leading to a factor proportional to $1/\kappa\mu$ where κ and μ are the force constant and reduced mass for the mode. A quantum mechanical treatment of the vibrational amplitude using harmonic oscillator ladder operators leads to a factor proportional to $1/\bar{\nu}_k$. Ozkabak et al. [3] and McCreery [18] neglect this amplitude factor, while Michalska and Wysokinski [17] use the $1/\bar{\nu}_k$ form (but they neglect the Boltzmann factor in the denominator).

Some common modifications to Eq. (2) might be: if a photon counting detector is used, the $(\bar{\nu}_0 - \bar{\nu}_k)^4$ should be replaced with $\bar{\nu}_0(\bar{\nu}_0 - \bar{\nu}_k)^3$ [18], and if 180° scattering is measured, the 7 should be replaced with a 4 [25]. Since we have restricted our study to the two a_{1g} stretching modes (since we can be very confident in their correct assignment), the $(\gamma')_k^2$ term is unimportant since it is zero for these totally symmetric vibrational modes; scattering geometry is not a factor for our study. Hence for every method studied, we converted the computed Raman activity into a corresponding intensity appropriate to our experimental conditions, then calculated the $I(\nu_1)/I(\nu_2)$ intensity ratio. We investigated the amplitude factor by considering the predicted intensity ratio computed with various methods and amplitude factors for benzene (Table 1).

Table 1 Comparison of experimental and computed intensity ratios in benzene: effect of vibrational amplitude factor

Method	Basis set	$I(\nu_1)/I(\nu_2)$, $Q_k^2 = 1$	$I(\nu_1)/I(\nu_2)$, $Q_k^2 = 1/\kappa\mu$	$I(\nu_1)/I(\nu_2)$, $Q_k^2 = 1/\bar{\nu}_k$
Experimental		0.91 ± 0.01	0.91 ± 0.01	0.91 ± 0.01
RHF	6-311 + g(3df,2p)	1.04	3.15	0.33
RHF	6-311 ++ g(3df,2p)	1.04	3.16	0.33
MP2	aug-cc-pVDZ	1.35	4.38	0.42
CCSD	aug-cc-pVDZ	1.45	4.19	0.46
B3LYP	6-311 + g(3df,2p)	1.46	4.45	0.46
CAS(6,6) 2p π	aug-cc-pVDZ	2.19	6.24	0.68

Table 2 Absolute Raman activities and comparison of experimental and computed intensity ratios in benzene: effect of computational method and basis set

Method	Basis set	$I(\nu_1)/I(\nu_2)$	Raman activity[a]	
Experimental		0.91 ± 0.01	ν_1	ν_2
RHF	6-311 + g(3df,2p)	1.04	351.1	93.7
RHF	6-311 ++ g(3df,2p)	1.04	352.1	93.9
RHF	6-31 ++ g(d)	1.16	372.0	87.0
RHF	6-31 + g(d)	1.17	371.5	86.1
MP2	aug-cc-pvdz	1.35	429.47	91.7
B3PW91	aug-cc-pvtz	1.44	417.0	86.0
CCSD	aug-cc-pvdz	1.45	398.9	80.5
B3LYP	6-311 + g(3df,2p)	1.46	410.9	84.1
BB1K [49]	MG3 [32]	1.47	405.4	79.6
MP2	6-31 + g(d)	1.52	416.6	79.3
B3LYP	6-31 + g(d)	1.58	428.2	79.8
PW91PW91	aug-cc-pvtz	1.62	454.1	86.5
MP2	cc-pvtz	1.82	400.0	63.4
CAS(6,6) π	aug-cc-pvdz	2.19	414.4	58.5
CAS(6,6) π	6-31g	3.66	382.6	27.9

[a]These are Raman activities in $Å^4\,amu^{-1}$ from the Gaussian output, except for the CAS and CCSD calculations where finite difference methods were used (see text). They are not corrected [with Eq. (2)] for laser frequency, temperature, or type of detector

The results in Table 1 make it clear that assuming a unit amplitude factor, as suggested by Ozkabak et al. [3] and McCreery [18] leads to significantly better agreement with carefully measured intensity ratios; this assumption will be adopted for the rest of this paper. Complete results for computed prediction of the intensity ratio for benzene are presented in Table 2.

There are three trends worth noting for the results in Table 2. (1) For any given method, the results generally improve with larger basis sets, and the inclusion of diffuse functions is particularly important, as noted by Ozkabak et al. [3]. It is highly likely that when the Sadlej [12,42,43] basis sets become generally available, the use of these with hybrid DFT methods will improve these results further. (2) Hartree–Fock seems to be superior to methods that include in various ways the electron correlation energy. (3) All of the methods tested overestimate the intensity of the C–H stretching mode compared to the C–C stretching mode. There appears to be somewhat more variation between methods and basis sets for the C–C Raman activity than for the C–H activity; neglecting the ν_2 Raman activity from the CAS calculation with the smallest basis set (which appears to be anomalously low), the relative standard deviations are about 7 and 12% for ν_1 and ν_2. The results do not suggest a dominant role for either the ν_1 or ν_2 Raman activity as a source for the overestimation of the intensity ratio. It is also clear from Table 2 that there is no benefit for predicting Raman intensities from treating the basis functions that contribute to the 6π MOs in a completely equivalent fashion as was done in the CAS(6,6) calculations.

Most of the methods in Table 2 were also applied to C_6D_6 and C_6F_6, except for the CAS(6,6) calculations (since they were quite poor for C_6H_6), and the CCSD calculations since they were prohibitively expensive for C_6F_6. Analogous results for these methods on two other species are shown in Table 3.

The results in Table 3 show that, like the case of C_6H_6, all of the methods tested overestimate the C–X stretching intensity compared to the C–C stretching intensity. They also suggest that Hatree–Fock with a large basis set is successful for C_6D_6, as it was for C_6H_6, but that it is quite poor for C_6F_6. Table 3 also makes it clear that none of these methods is very good for C_6F_6. It seems that accurate prediction of the intensity of both the most intense, and one of the least intense bands in the Raman spectrum is still quite challenging. The PW91PW91/aug-cc-pvtz calculations are much better than the others, overestimating the C–F stretching intensity by only 80% compared to the C–C stretching intensity; unfortunately this method was rather poor for C_6H_6 and C_6D_6.

Table 3 Comparison of experimental and computed intensity ratios in C_6D_6 and C_6F_6: effect of computational method and basis set

Method	Basis set	$I(\nu_1)/I(\nu_2)$ C_6D_6	$I(\nu_1)/I(\nu_2)$ C_6F_6
Experimental		0.646 ± 0.004	0.0178 ± 0.0003
RHF	6-311+g(3df,2p)	0.662	0.140
RHF	6-31+g(d)	0.776	0.134
MP2	aug-cc-pvdz	0.860	0.073
B3PW91	aug-cc-pvtz	0.908	0.060
B3LYP	6-311+g(3df,2p)	0.920	0.065
BB1K(X)	MG3(Y)	0.943	0.106
MP2	6-31+g(d)	0.984	0.089
PW91PW91	aug-cc-pvtz	1.009	0.032
B3LYP	6-31+g(d)	1.021	0.066
MP2	cc-pvtz	1.182	0.085

4 Discussion

It is quite unexpected that the Hartree–Fock methods seem to be superior to methods that include the electron correlation energy for predicting Raman intensity in C_6H_6. We suspect that this unexpected result is due to a fortuitous cancellation of errors. It is possible that this cancellation involves the highly anharmonic nature of the C–H stretching modes. It is important to recall that since the automatic Raman activities in Gaussian are computed on the assumption of harmonic vibrations, and the derivation of Eq. (2) is also based on the assumption of both electrical and mechanical harmonicity, it may be that neglecting anharmonicity may cancel some of the error in neglecting electron correlation energy. Indeed, Maslen et al. [44] have shown that at the Hartree–Fock level, anharmonic corrections to Raman intensity are quite small, but they make no claim that this will be the case for the electron correlated methods. The ground state anharmonicities of C_2, CH, CD, and CF are 13.34 cm^{-1} [45], 63.02 cm^{-1} [46], 34.02 cm^{-1} [47], and 11.10 cm^{-1} [48], respectively, so it is reasonable to expect that the C–H bond stretching vibrations are the most anharmonic in this study. We are investigating methods to develop an intensity formula like Eq. (2) that does not depend on the assumption of mechanical harmonicity.

It should be noted (Fig. 2) that ν_1 for C_6F_6 occurs at 1,492 cm^{-1} and $2\nu_7$ occurs at 1,433 cm^{-1}; since this overtone has a_{1g} symmetry there is a possibility of Fermi resonance between these modes. If they were in resonance the position of the overtone would be shifted away from ν_1, relative to twice the frequency of the fundamental (ν_7), and the intensity of the overtone would be enhanced at the expense of intensity in the adjacent fundamental, ν_1. If such a Fermi resonance occurred, the experimental band intensity at 1,492 cm^{-1} could not be easily compared to computed values. Laposa and Montogomery [39] have assigned ν_7 at 714 cm^{-1}; this suggests that $2\nu_7$ should be at 1,428 cm^{-1}. Since we observed this at 1,433 cm^{-1}, the shift is trivially small, and in the wrong direction, for any significant Fermi resonance perturbation of the ν_1 intensity at 1,492 cm^{-1}. A future publication will compare in detail the vibrational spectra of C_6F_6 and $^{13}C_6F_6$ and this Fermi resonance possibility will be addressed in detail based on isotopic shifts.

With the methods described here, it is possible to simulate the entire Raman spectrum from the activities computed by Gaussian. Equation (2) may be used to convert these activities into the corresponding intensities predicted for a given sample temperature, laser frequency, and type of detector. A simple way to do this is to assume that all of the Raman bands will be described by Lorentzian peaks with a common width, whose areas are proportional to the predicted intensity. Figure 5 shows such a simulation for the complete Raman spectrum of C_6D_6, using the results from a calculation at the RHF/6-311+g(3df,2p) level of theory.

In this figure all of the predicted frequencies were scaled so that the predicted and observed ν_1 frequencies would match; the predicted intensities were scaled so that the ν_1 intensities would match; then a common peak width for all of the Lorentzians was chosen so that the ν_1 lineshapes would match as closely as possible. The black curve represents the experimental intensity, corrected for spectrometer response; the blue curve is the predicted Raman *intensity*; and the red

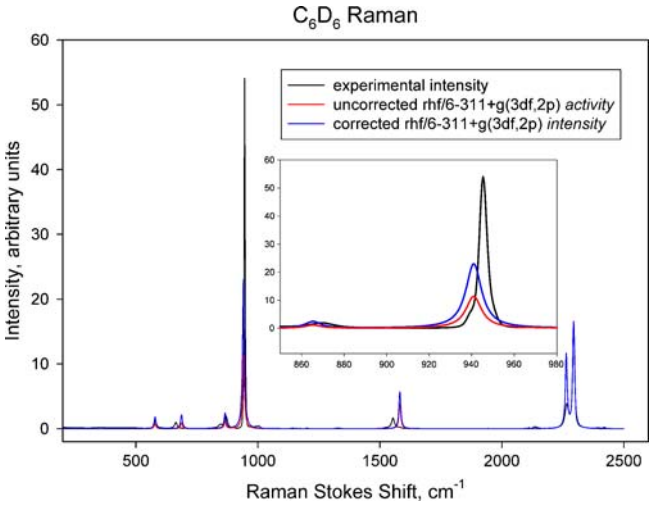

Fig. 5 Experimental Raman spectrum of C_6D_6 with intensities corrected for spectrometer response (*black*); theoretical Raman spectra at the RHF/6-311+g(3df,2p) level with frequencies, peak widths, and peak heights scaled to match experiment at ν_1: theoretical Raman *activity* (*red*), theoretical Raman *intensity* (*blue*) with activities corrected for experimental conditions: temperature, laser frequency, and type of detector

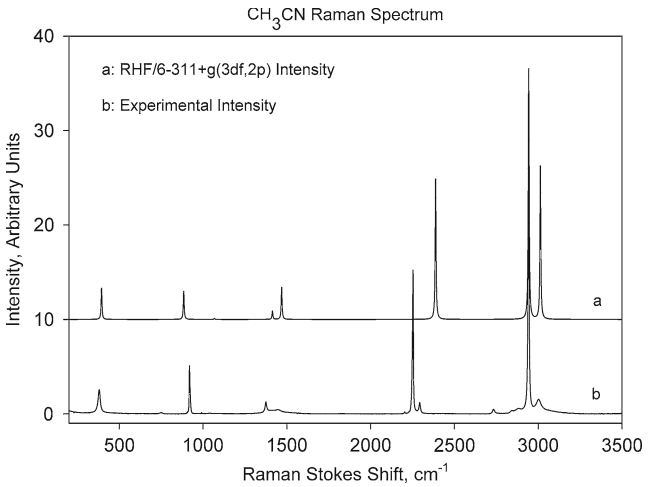

Fig. 6 Raman Spectra of CH_3CN. **a** Simulated spectrum based on RHF/6-311+g(3df,2p) activities corrected for laser frequency, temperature, and power detector. Frequencies were scaled by 0.9215 and Lorentzians with 3 cm^{-1} width were used; intensities shifted up by 10 units. **b** Experimental spectrum with intensities corrected for spectrometer response

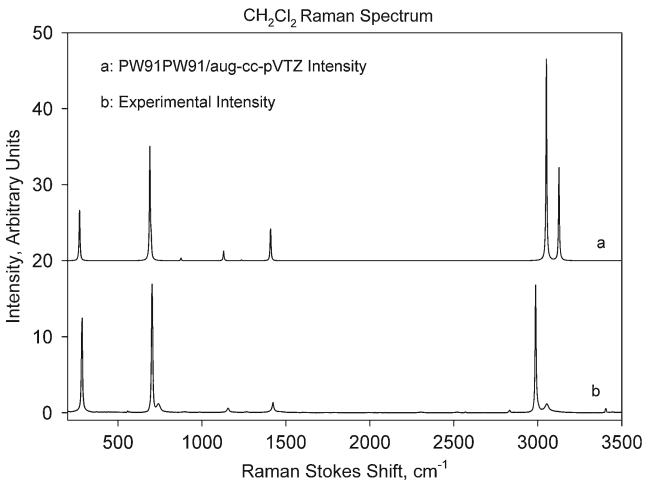

Fig. 7 Raman Spectra of CH_2Cl_2. **a** Simulated spectrum based on PW91PW91/aug-cc-pVTZ activities corrected for laser frequency, temperature, and power detector. Frequencies were not scaled and Lorentzians with 3 cm^{-1} width were used; intensities shifted up by 20 units. **b** Experimental spectrum with intensities corrected for spectrometer response

curve is the predicted Raman *activity*, uncorrected for laser frequency, temperature, and type of detector. The inset clearly shows that such correction is quite important; the area under the blue curve is nearly equal to that under the black curve, but they have different peak widths. The red curve has significantly smaller area.

Figures 6 and 7 show similar comparisons of simulated and experimental Raman spectra for CH_3CN and CH_2Cl_2. The simulations were based on RHF/6-311+g(3df,2p) calculated Raman activities (CH_3CN) and PW91PW91/aug-cc-pVTZ activities (CH_2Cl_2).

5 Conclusions

For predicting the Raman intensities for hydrocarbons we recommend the use of Hartree–Fock calculations with a large basis set including diffuse functions. For other types of molecules, or where C–H stretching intensity is not of interest, perhaps a DFT method such as PW91PW91 with a basis set including diffuse functions would be better. This latter choice has the advantage that it will also produce more accurate vibrational frequencies than will the Hartree–Fock calculations.

Acknowledgements A portion of the research described in this manuscript was performed at the W.R. Wiley Environmental Molecular Sciences Laboratory, a national scientific user facility sponsored by the US Department of Energy's Office of Biological and Environmental Research and located at the Pacific Northwest National Laboratory. PNNL is operated for the Department of Energy by Battelle. We thank Dr. Jürgen Sawatzki of Bruker Optik for assistance with the polarization measurements. Computer time was supported by collaborative hpc resources funded through the University of North Carolina Office of the President.

References

1. Scott AP, Radom LJ (1996) J Phys Chem 100:16502, http://srdata.nist.gov/cccbdb/vsf.asp (accessed 8/13/2004)
2. Kormornicki A, McIver JW (1979) J Chem Phys 70:2014
3. Ozkabak AG, Thakur SN, Goodman L (1991) Int J Quantum Chem 39:411
4. Tai S, Papasavva S, Kenny JE, Gilbert BD, Janni JA, Steinfeld JI, Taylor JD, Weinstein RD (1999) Spectrochim Acta Part A 55:9
5. Furlan A, Fischer T, Fluekiger P, Güdel HU, Leutwyler S, Lüthi HP, Riley MJ, Weber J (1992) J Phys Chem 96:10713
6. Johnson BG, Florian J (1995) Chem Phys Lett 247:120
7. Stirling A (1996) J Chem Phys 104:1254
8. Kozlowski PM, Rauhut G, Pulay P (1995) J Chem Phys 103:5650
9. Kozlowski PM, Jarzecki AA, Pulay P, Li XY, Zgierski MZ (1996) J Phys Chem 100:13985
10. Shinohara H, Yamakita Y, Ohno K (1998) J Mol Struct 442:221
11. Wojciechowski PM, Zierkiewicz W, Michalska D, Hobza P (2003) J Chem Phys 118:10900
12. Oakes RE, Bell SEJ, Benkova Z, Sadlej AJ (2005) J Comp Chem 26:154
13. Oakes RE, Beattie JR, Moss BW, Bell SEJ (2002) J Mol Struct (Theochem) 586:91
14. Oakes RE, Beattie JR, Moss BW, Bell SEJ (2003) J Mol Struct (Theochem) 626:27
15. Oakes RE, Spence SJ, Bell SEJ (2003) J Phys Chem A 107:2964
16. Oakes RE, Bell SEJ (2003) J Phys Chem A 107:10953
17. Michalska D, Wysokinski R (2005) Chem Phys Lett 403:211
18. McCreery RL (2002) In: Chalmers JM, Griffiths, PR (eds) Handbook of Vibrational Spectroscopy, Vol 1, Wiley, New York, pp 920–932
19. Johnson TJ, Sams RL, Blake TA, Sharpe SW, Chu PM (2002) Appl Opt 41:2831
20. Bertie JE (1998) Pure Appl Chem 70:2039
21. Schrader B, Hoffmann A, Simon A, Podschadlowski R, Tischer M (1990) J Mol Struct 217:207
22. Chase DB (1986) J Am Chem Soc 108:7485
23. Sharpe SW, Johnson TJ, Sams RL, Chu PM, Rhoderick GC, Johnson PA (2004) Appl Spec 58:1452
24. Rothman LS (2003) J Quant Spectrosc Radiat Transf 82:5
25. Long DA (1977) Raman spectroscopy. McGraw-Hill, New York
26. Hoffmann A, Keller S, Schrader B, Ferwerda R, van der Maas JH (1991) J Raman Spectrose 22:497

27. Schrader B, Hoffmann A, Simon A, Sawatzki J (1991) Vib Spectrosc 1:239
28. Angel RJ (2003) J Appl Crystallogr 36:295
29. Fernandez-Sanchez JM, Murphy WF (1994) Chem Phys 179:479
30. Gaussian 98, Revision A.9, Frisch MJ, Trucks GW, Schlegel HB, Scuseria GE, Robb MA, Cheeseman JR, Zakrzewski VG, Montgomery JA Jr, Stratmann RE, Burant JC, Dapprich S, Millam JM, Daniels AD, Kudin KN, Strain MC, Farkas O, Tomasi J, Barone V, Cossi M, Cammi R, Mennucci B, Pomelli C, Adamo C, Clifford S, Ochterski J, Petersson GA, Ayala PY, Cui Q, Morokuma K, Malick DK, Rabuck AD, Raghavachari K, Foresman JB, Cioslowski J, Ortiz JV, Baboul AG, Stefanov BB, Liu G, Liashenko A, Piskorz P, Komaromi I, Gomperts R, Martin RL, Fox DJ, Keith T, Al-Laham MA, Peng CY, Nanayakkara A, Challacombe M, Gill PMW, Johnson B, Chen W, Wong MW, Andres JL, Gonzalez C, Head-Gordon M, Replogle ES, Pople JA (1998) Gaussian, Inc., Pittsburgh
31. Gaussian 03, Revision B.04, Frisch MJ, Trucks GW, Schlegel HB, Scuseria GE, Robb MA, Cheeseman JR, Montgomery JA Jr, Vreven T, Kudin KN, Burant JC, Millam JM, Iyengar SS, Tomasi J, Barone V, Mennucci B, Cossi M, Scalmani G, Rega N, Petersson GA, Nakatsuji H, Hada M, Ehara M, Toyota K, Fukuda R, Hasegawa J, Ishida M, Nakajima T, Honda Y, Kitao O, Nakai H, Klene M, Li X, Knox JE, Hratchian HP, Cross JB, Adamo C, Jaramillo J, Gomperts R, Stratmann RE, Yazyev O, Austin AJ, Cammi R, Pomelli C, Ochterski JW, Ayala PY, Morokuma K, Voth GA, Salvador P, Dannenberg JJ, Zakrzewski VG, Dapprich S, Daniels AD, Strain MC, Farkas O, Malick DK, Rabuck AD, Raghavachari K, Foresman JB, Ortiz JV, Cui Q, Baboul AG, Clifford S, Cioslowski J, Stefanov BB, Liu G, Liashenko A, Piskorz P, Komaromi I, Martin RL, Fox DJ, Keith T, Al-Laham MA, Peng CY, Nanayakkara A, Challacombe M, Gill PMW, Johnson B, Chen W, Wong MW, Gonzalez C, Pople JA (2003) Gaussian, Inc., Pittsburgh
32. Fast PL, Sanchez ML, Truhlar DG (1999) Chem Phys Lett 306:407
33. Curtiss LA, Redfern PC, Raghavachari K, Rasslov V, Pople JA (1999) J Chem Phys 110:4703
34. Curtiss LA, Raghavachari K, Redfern PC, Rasslov V, Pople JA (1998) J Chem Phys 119:7764
35. Kendall RA, Dunning TH Jr, Harrison RJ (1992) J Chem Phys 96:6796
36. Herzberg G (1945) Molecular spectra and molecular structure II. Infrared and Raman spectra of polyatomic molecules. Van Nostrand Reinhold, New York
37. Fernandez-Sanchez JM, Montero S (1989) J Chem Phys 90:2909
38. Delbouille L (1956) J Chem Phys 25:182
39. Laposa JD, Montgomery C (1982) Spectrochim Acta 38A:1109
40. Yumura T, Koga M, Hoshikawa H, Nibu Y, Shimada R, Shimada H (1998) Bull Chem Soc Jpn 71:349
41. Suzuki Y, Shimada H, Shimada R (1996) Bull Chem Soc Jpn 69:3081
42. Benkova Z, Sadlej AJ, Oakes RE, Bell SEJ (2005) J Comput Chem 26:145
43. Benkova Z, Sadlej AJ, Oakes RE, Bell SEJ (2005) Theor Chem Acc 113:238
44. Maslen PE, Handy NC, Amos RD, Jayatilaka D (1992) J Chem Phys 97:4233
45. Ballik EA, Ramsay DA (1963) Astrophys J 84:137
46. Rydbeck OEH, Ellder J, Irvine WM (1973) Nature (London) 246:466
47. Huber KP, Herzberg G (2005) Constants of diatomic molecules (data prepared by Gallagher JW, Johnson RD, III) In: Linstrom PJ, Mallard WG (eds) NIST Chemistry WebBook, NIST standard reference database number 69. June 2005, National Institute of Standards and Technology, Gaithersburg MD, 20899 (http://webbook.nist.gov)
48. Carrington A, Howard BJ (1970) Mol Phys 18:225
49. Zhao Y, Lynch BJ, Truhlar DG (2004) J Phys Chem 108:2715